Mathematical analysis of a batch electrocoagulation reactor

P.K. Holt*, G.W. Barton* and C.A. Mitchell**

* Department of Chemical Engineering, University of Sydney, Australia
(E-mail: *pholt@chem.eng.usyd.edu.au*)

** Institute for Sustainable Futures, UTS, Australia

Abstract Electrocoagulation treats water by delivering coagulant from a sacrificial anode (aluminium) in an electrochemical cell. Hydrogen is evolved from the inert cathode. In the batch electrocoagulation reactor numerous interactions occur with settling and flotation identified as the dominant removal paths. Current determines both coagulant dosage and bubble production rate. The bubbles influence the mixing, and hence mass diffusion within the reactor. Rate of flotation and settling were experimentally determined for currents 0.25–2.0 A and pollutant loading 0.1–1.7 g/L. The performance of the electrocoagulation reactor was quantified by analysis of experimental results.

First-order ordinary differential equations were developed to describe the pollutant's settling and flotation behaviour. Kinetic rate constants were calculated considering this pair of irreversible reactions. At low current (0.25A), sedimentation dominates with slow release of coagulant and gentle agitation provided by low bubble production. Removal is slow and hence the low rate constants calculated were appropriate. At high currents (1.0 and 2.0 A) faster removal occurs due to greater bubble density. This resulted in greater mass floated to the surface and higher rate constants were observed. Thus the developed rate equations successfully quantified the reactor's performance over a variety of conditions.

Keywords Electrocoagulation; mathematical analysis; water

Introduction

Towards the end of the nineteenth century, electrocoagulation was seen as a promising water cleansing technology. A treatment plant was successfully commissioned in London at this time (Matteson *et al*., 1995). In the following decades, plants were also commissioned in the United States to treat municipal wastewater. Vik *et al*. (1984) report that by the 1930s all such plants had been abandoned due to perceived higher operating costs and the ready availability of mass-produced alternatives for chemical coagulant dosing.

In recent years, however, smaller-scale electrocoagulation processes have found a niche in the water treatment industry, proving to be reliable and effective technologies, though requiring greater technical understanding for their potential to be fully exploited. Only recently has research aimed at a quantitative understanding of electrocoagulation's relatively complex pollutant removal mechanisms (Holt *et al*., 1999).

Electrocoagulation is a complex process, with a multitude of mechanisms operating synergistically to remove pollutants from the water. A diversity of opinions exist in the literature for explaining both the key mechanisms and the best reactor configurations. Design variations include a fluidised-bed reactor employing aluminium pellets (Barkley *et al*., 1993), bipolar aluminium electrodes (Mameri *et al*., 1998), mesh electrodes (Matteson *et al*., 1995), as well as simple plate electrodes (Vik *et al*., 1984; Pouet *et al*., 1995). There is certainly no dominant "electrocoagulation reactor" in use. Reported operating conditions and performance mirror the wide variation in design, with reactors invariably being "tuned" to best suit a specific application. These empirical approaches invariably prove the viability of the technology, but singularly fail to fully capitalise on its potential. This is due

Water Science and Technology: Water Supply **Vol 2 No 5–6 pp 65–71**

to a lack of fundamental understanding of the system and hence the inability to accurately predict performance.

Figure 1 begins to show the complex, interdependent nature of the electrocoagulation process (Holt *et al*., 1999, 2001). A sacrificial metal anode (usually aluminium, but sometimes iron) is used to dose polluted water with a coagulating agent. Simultaneously, electrolytic gases (mainly hydrogen at the cathode) are generated. There are numerous interactions occurring including, aqueous speciation, precipitation, particle-particle interactions, particle-bubble interactions, aggregation, settling and flotation to name a few processes. These numerous pollutant removal paths, interactions and the complexity of electrocoagulation create a challenging process to model mechanistically.

The basis of electrocoagulation is formed by three separate categories of mechanistic processes – electrochemistry, coagulation and flotation. These processes are difficult to investigate separately in an operational reactor, which goes some way towards explaining the lack of a detailed technical literature and modelling on electrocoagulation.

An investigation by Matteson *et al*. (1995) focused on the coagulation aspects of electrocoagulation. They recognized the production of electrolytic gases were significant at both electrodes but did not include flotation effects in their second-order model. Mameri *et al*. (1998) derived a first-order model for the removal of fluoride from water and similarly did not include flotation effects. Recent work by Holt *et al*. (2001) identified settling and flotation as the main removal paths. Previous electrocoagulation models considered only the coagulation process and removal by settling, neglecting flotation and electrochemistry. This paper includes the flotation effect in addition to coagulation and aims to present a consistent mathematical analysis using experimental data.

Experimental method

The batch electrocoagulation reactor used is constructed of Perspex and has a maximum capacity of 7.1 L previously described by Holt *et al*. (2001). The pollutant used was a "potter's clay", comprising kaolinite (67%), quartz (25%), illite/mica (3%), feldspar (3%) and other trace elements (2%), as characterised by X-ray diffraction analysis.

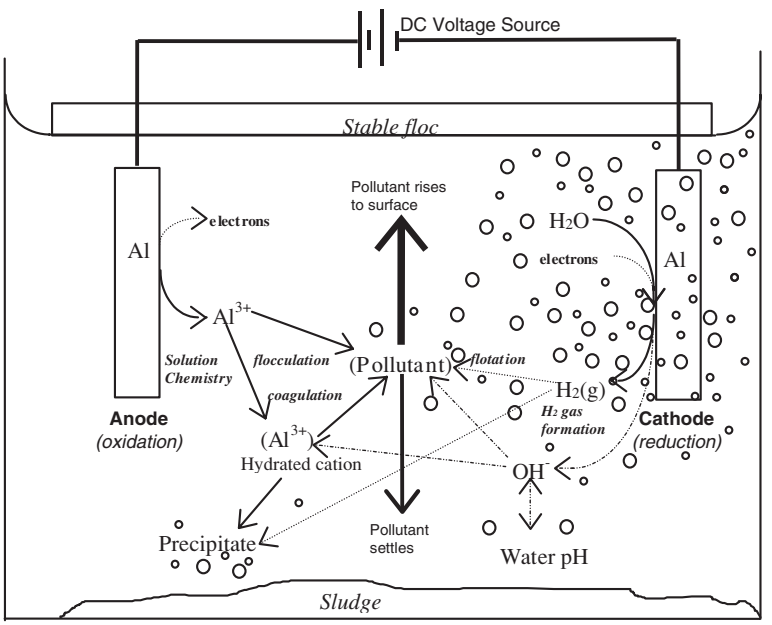

Figure 1 Interactions occurring within an electrocoagulation reactor

The electrode arrangement consists of five stainless steel cathodes interspersed with four aluminium anodes, with brass rods used to connect the parallel plate electrodes. The current was held constant for each run. The series of experimental runs investigated the effect of current over the range 0.25 to 2.0A and initial pollutant loading from 0.1 to 1.7 g/L.

Mass (clay and coagulant) balances were conducted over the reactor. A scraper was used to collect the froth/foam containing pollutant at the surface, which was then funnelled to a beaker. Froth at the surface was collected at regular intervals (usually every five minutes), dried and weighed. At the conclusion of the experiment, the solid sludge at the base of the reactor was also collected, dried and weighed.

Settling experiments for clay (no coagulant) were carried out in measuring cylinders, with the level of water filled to the same height as the reactor (155mm). Particle size distribution was measured using a Malvern Mastersizer S with coarser particles (> 53 μm) separated using sieves.

Results

Settling results for clay without coagulant additions are shown in Figure 2. There is a good correlation between the mass of clay settled (data points) and that predicted by Stokes law (solid line). Typical experiments began approximately five minutes after addition of clay, allowing large particles to settle. Larger particles settled rapidly with the fraction > 24 μm settling in less than 5 minutes. Hence approximately 41% of the mass of clay added settled before electrocoagulation commenced. Further settling occurs in an approximately linear region of the settling curve and hence can be characterised by a linear relationship.

The settling characteristic of clay shown in Figure 2 provides a base line for comparison of the effect of electrocoagulation. After electrocoagulation at 0.25 A, the mass at the base of the electrocoagulation reactor increased compared with the untreated clay as shown in Table 1 indicating enhanced settling. At higher currents, 1.0 and 2.0 A, the settling of clay is hindered resulting in less mass settling and a greater amount recovered at the surface.

Table 1 Mass settled (%) with and without electrocoagulation for initial pollutant loading of 1.7 g/L

Current (A)	Time (hours)	Without electrocoagulation	With electrocoagulation
0.25	3	64%	86%
1.0	1	55%	47%
2.0	1	55%	40%

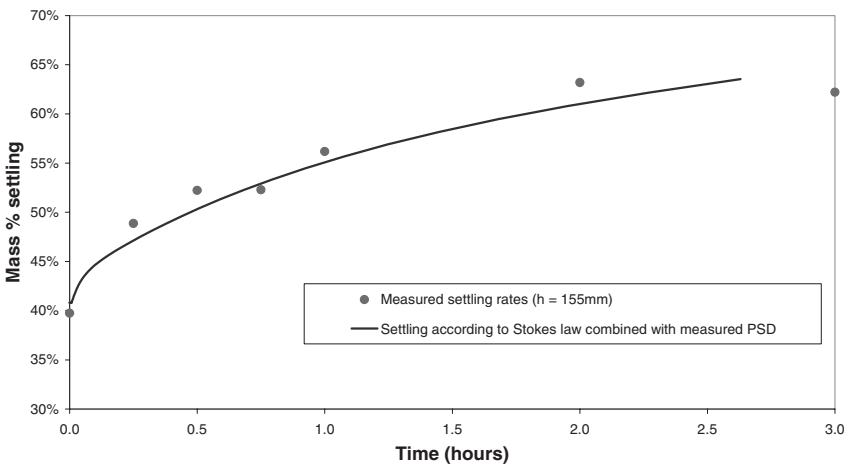

Figure 2 Settling curve of clay pollutant measured at selected times (points) and calculated using Stokes law combined with measure particle size distribution (line)

Mass (other than water) in the reactor comes from either the clay added initially or from material generated by the electrodes. The amount of aluminium and hydroxide ions generated can be calculated using Faraday's law (Eq. (1)), where the mass (m) in grams of a species oxidised or reduced at a specific current (I) (A) and period of time (t) (s) can be deduced as follows,

$$m = \frac{I \times t \times MW}{ZF} \tag{1}$$

where Z is the number of electrons transferred, MW is the molecular weight (g mol^{-1}) and F is Faraday's constant (96,486 C mol^{-1}).

As noted, mass was collected at both the surface and base of the reactor. Thus, the mass balance is:

Mass **IN** (FEED)	+	Mass **IN** (GENERATED)	=	Mass **OUT** (SURFACE)	+	Mass **OUT** (BASE)	+	Mass **REMAINING** (BULK SOLUTION)	(2)
clay		*Aluminium hydroxide*		*collected*		*collected*			

Clay concentration, shown in Figure 3, was calculated assuming clay settled linearly over the reaction time and all aluminium hydroxide formed from electrodes precipitated. Mass remaining "in solution" consistently accounted for less than 2% of the total mass, indicating tight closure of the mass balance. At low initial pollutant loading (0.1 g/L) the concentration profile in Figure 3 is essentially flat. At this low concentration, experimental error in collection of mass at the surface becomes significant and thus the results are not included for further analysis.

Analysis of data

In this electrocoagulation reactor, the clay pollutant is either removed by sedimentation or flotation to the surface. The controlling parameter is the electrical current as it determines both the production of coagulant (aggregation) and bubbles (flotation) (Holt *et al.*, 2001). Consequently the two removal mechanisms occur simultaneously, competing for the clay pollutant. The relationship between separation processes can be mathematically described by two irreversible reactions in parallel. The first for removal to the surface (flotation – equation 3) and the second removal to the base (sedimentation – Eq. (4)) (Levenspiel, 1999).

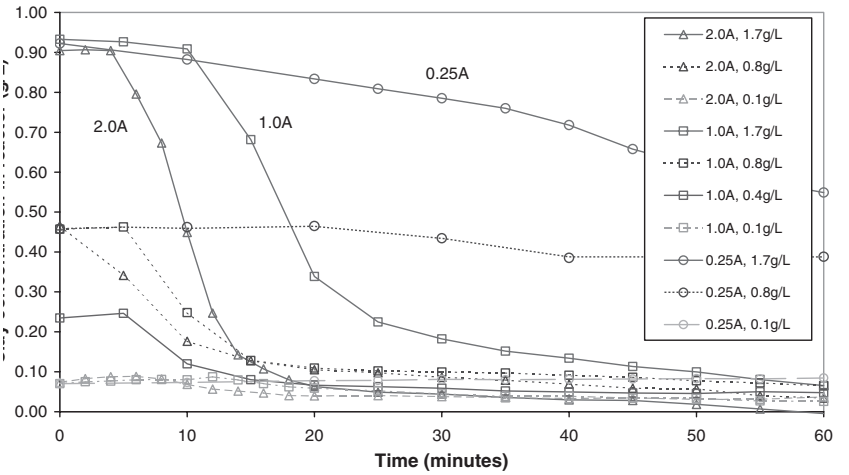

Figure 3 Bulk solution pollutant concentration at currents 0.25, 1.0 and 2.0 A and initial pollutant loadings 0.1, 0.4, 0.8 and 1.7 g/L

$$P \xrightarrow{k_1} S \tag{3}$$

$$P \xrightarrow{k_2} B \tag{4}$$

where the pollutant (P) follows first-order removal kinetics to either the surface (S) or the base (B) of the reactor. The rate equations for each species can be expressed in terms of their concentrations.

$$-r_P = -\frac{dc_P}{dt} = k_1 c_P + k_2 c_P = (k_1 + k_2) c_P \tag{5}$$

$$r_S = \frac{dc_S}{dt} = k_1 c_P \tag{6}$$

$$r_B = \frac{dc_B}{dt} = k_2 c_B \tag{7}$$

where c_P is the concentration of the pollutant in the bulk solution and c_S and c_B are the theoretical "concentrations" at the surface and at the base respectively relative to the bulk solution. Thus a series of ordinary differential equations describe the behaviour of the electrocoagulation reactor.

A time lag (t_{lag}) enabling a critical coagulant concentration to be attained that is dependent on current, exists before the electrocoagulation reaction proceeds (Holt *et al.*, 2001). Thus integrating Eq. (5) from t_{lag} to t and c_P^0 to c_P.

$$-\ln\left(\frac{c_P}{c_P^0}\right) = (k_1 + k_2)(t - t_{lag}). \tag{8}$$

Dividing Eq. (6) by 7 and integrating.

$$\frac{c_S - c_S^0}{c_B - c_B^0} = \frac{k_1}{k_2} \tag{9}$$

Plotting the left-hand side of Eq. (8) against (t–t_{lag}) and fitting a linear equation to the data determines the slope, (k_1+k_2) as shown in Figure 4. Figure 5 plots the "concentration" at the base against the surface and fitting a linear equation to the data determines the

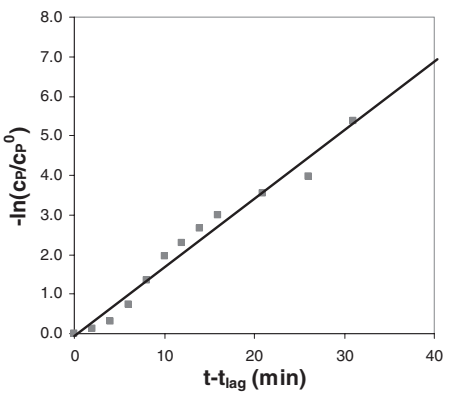

Figure 4 Evaluation of k_1+k_2 for 2.0 A with initial clay pollutant loading of 2.0 g/L

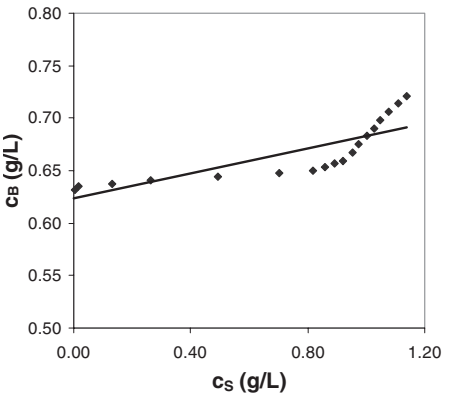

Figure 5 Evaluation of k_1/k_2 for 2.0 A with initial clay pollutant loading of 2.0 g/L

slope, (k_1/k_2). The combination of these results enables the rate constants (k_1 and k_2) to be determined.

The rate constants for removal to the surface, k_1, and settling, k_2, are presented in Figure 6 and 7 respectively. At higher current, the rate constant is higher, as would be expected as the coagulant addition and bubble production rates are higher.

The rate constants for the mass settling (k_2) do not follow a linear path increasing at a greater rate than would be expected. A higher removal rate constant than expected is observed at initial pollutant loading of 1.7 g/L and 2.0 A. This suggests more complex interactions occur which the first-order model does not adequately describe.

Discussion

Current has dual effect; firstly it determines the coagulant addition rate and secondly, the production rate of electrolytic gases. The gases not only provide a flotation removal pathway but also agitate the solution thereby increasing the diffusion of pollutant and coagulant (Holt *et al.*, 2001).

At low operating current (0.25 A), settling is the dominant removal mechanism where the response of the system is much slower as observed by the gradual change in the pollutant concentration profile as shown in Figure 3. Few bubbles are produced resulting in a decrease in mixing and material uplift. The coagulant dosage rate is low and combined with gentle agitation settling is favoured. The total settling is enhanced compared to untreated clay with a total 86% of the mass being collected at the reactor's base (for initial pollutant loading 1.7 g/L). Operation at low current results in low rate constants for both removal by flotation and settling (Figures 6 and 7).

As current increases so does the bubble density, increasing the upward momentum lift. This resulted in a greater percentage of mass being removed at the surface with the highest

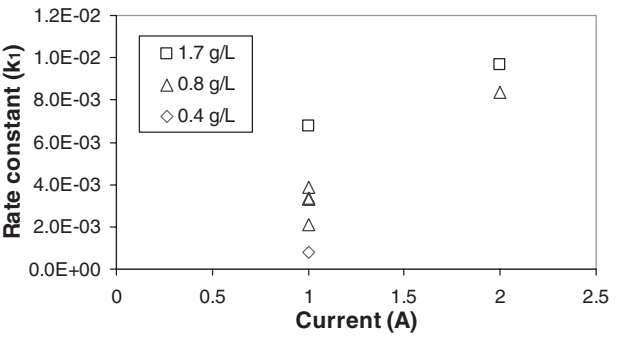

Figure 6 Rate constant (k_1) for surface with initial clay pollutant loading of 1.7, 0.8 and 0.4 g/L

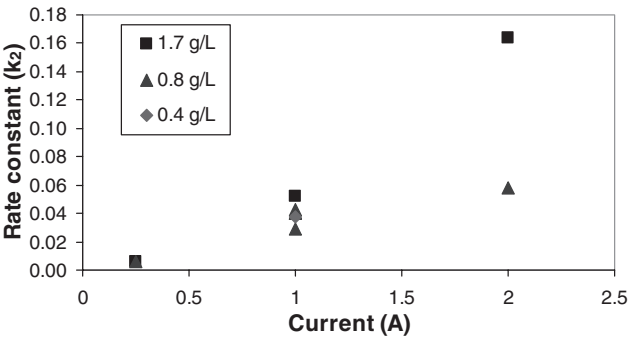

Figure 7 Rate constant (k_2) for base with initial clay pollutant loading of 1.7, 0.8 and 0.4 g/L

current, 2 A, reporting 60% of the mass to the surface. A faster removal is observed by the sharp decline in the clay concentration profile and the shorter time lag shown in Figure 3. This trend is reflected by the increase of the rate constants with current.

The first-order model appears appropriate for the removal by flotation with the rate constant to the surface k_1 increasing from 7×10^{-3} to 1×10^{-2} as the current is doubled from 1.0 to 2.0 A for initial pollutant loading of 1.7 g/L. The rate constant appears to be sufficiently described by a function of current and pollutant loading. In contrast, the removal rate at the base (k_2) increases from 0.05 to 0.16 as current is doubled for the same pollutant loading. This large increase of k_2 with current implies a more complex relationship to its removal. Further investigation is required to decipher more appropriate removal mechanisms.

The electrocoagulation system can be operated to direct mass to the surface (flotation) or to the base (sedimentation). Major trends of the electrocoagulation reactor are reflected by the combination of first order rate equations (Eqs (5)–(7)). At low current, removal kinetics are slow increasing as currents increases. Reproducibility of the results is shown by the four repetitions at 1 A and 0.8 g/L (triangles) and is acceptable to a first approximation.

Conclusion

The mathematical analysis of experimental data is reproducible and quantifies the behaviour of the electrocoagulation reactor to a first approximation. The ordinary differential rate equations developed follow the major trends of pollutant removal. At high current, flotation is the major removal mechanism whilst settling dominants at low current and this trend is reflected by the rate constants.

References

Barkley, N.F. *et al*. (1993). Alternating current electrocoagulation for Superfund site remediation. *Air and Waste*, **43** (May).

Holt, P.K. *et al*. (1999). *Electrocoagulation as a wastewater treatment*. Third Annual Australian EERE, Victoria.

Holt, P.K. *et al*. (2001). *A step forward to understanding electrocoagulation, characterisation of pollutant's fate*. 6th World Congress of Chemical Engineering, Melbourne, Australia.

Levenspiel, O. (1999). *Chemical Reaction Engineering*. New York, John Wiley and Sons.

Mameri, N. *et al*. (1998). Defluoridation of septentrional Sahara water of North Africa by electrocoagulation process using bipolar aluminium electrodes. *Water Research*, **32**(5), 1604–1612.

Matteson, M.J. *et al*. (1995). Electrocoagulation and separation of aqueous suspensions of ultrafine particles. *Colloids and Surfaces A: Physicochemical and Engineering Aspects*, **104**(1), 101–109.

Pouet, M.F. *et al*. (1995). Urban wastewater treatment by electrocoagulation and flotation. *Water Science and Technology*, **31**(3–4), 275–283.

Vik, E.A. *et al*. (1984). Electrocoagulation of potable water. *Water Research*, **18**(11), 1355–1360.